2 PERKIN

Theoretical characterization of pentazole anion with metal counter ions. Calculated and experimental ^{15}N shifts of aryldiazonium, -azide and -pentazole systems †

Luke A. Burke,*[a] Richard N. Butler *[b] and John C. Stephens [b]

[a] *Department of Chemistry, Rutgers the State University of New Jersey, Camden, NJ08102, USA*
[b] *Chemistry Department, National University of Ireland, Galway, Ireland*

Received (in Cambridge, UK) 30th April 2001, Accepted 12th June 2001
First published as an Advance Article on the web 26th July 2001

Theoretical studies of proposed structures for NaN_5, KN_5, $Mg(N_5)_2$, $Ca(N_5)_2$, and $Zn(N_5)_2$ metal complexed pentazole anions have been carried out with the RHF, MP2, MCSCF, and DFT theoretical methods. Additional DFT calculations were performed on MgN_5Cl, CaN_5Cl, and ZnN_5Cl pentazoles. The structures considered are unidentate **I**, bidentate **II**, and metallocene-like **III**. For Mg, Na, K, and Ca pentazoles at every level of theory, **II** is the most energetically favoured, followed by **I**, then **III**. Complex **I** is preferred with Zn complexes due to favourable d orbital interactions. For double ring complexes only **II** (**I** for Zn) with perpendicular rings has all positive vibrational frequencies. For single ring complexes, both **II** (**I** for Zn) and **III** have all positive vibrations. Structure **I** (**II** for Zn) is a transition state structure for metal ion rotation around the ring (E_a 5–10 kcal mol^{-1}). N atom chemical shifts relative to NH_3 and nitromethane were calculated for each species using the lowest energy configuration and the B3LYP//6-311++G(2d,p) method on the B3LYP//6-31G(d) optimised geometry. Additional calculations were done for 1-arylpentazoles, 1-arylpentazene, aryl azides, and aryldiazonium ions. Calculated ^{15}N NMR shifts were within 20 ppm of experiment. Time dependent B3LYP/6-31G(d) and B3LYP/6-311+G(d) calculations were performed on all stable species. All $^1(\pi,\pi)$ transitions were calculated to be below 180 nm, while the $^1(n,\pi)$ transitions were below 210 nm. The lowest energy transitions are from the lone pairs to the empty metal s orbital. For Mg and Zn these transitions are at ~220 nm. For Na, Ca and K the transitions are considerably lower in energy, ~250 nm.

Introduction

Substituted 1-arylpentazoles have been synthesised and characterised for over forty years.[1] There have been no reports yet of the preparation of the parent pentazole HN_5 or its metal salts. We report here the results of theoretical calculations on pentazole anion and various metal cation–pentazole anion complexes in terms of their structures, vibrational frequencies, electronic transitions, and ^{15}N chemical shifts. Metallocene-like structures have been proposed[2] but no studies have appeared where vibrational frequencies have been calculated in order to characterise the structures as first or higher order transition states. Yet another structure (Scheme 1) could be expected based on the known aryl substituted pentazole structure.[1–3]

Scheme 1

In the case of Na^+ and K^+, there is only substitution to one ring. For the divalent Mg^{2+}, Ca^{2+}, and Zn^{2+} ions there is possible substitution by two rings or by one ring and another anion. For the purposes of this study, we have chosen the former for an analysis by different levels of theory and the latter only by Density Functional Theory (DFT). In exploring the hypersurfaces, three principal structures were found (Scheme 2, N at all corners). They are **I**, with one point of attachment to the ring (unidentate), **II** two points (bidentate), and **III** centrally over the ring (metallocene-like). In the double rings, the rings can rotate from (D_{2d}) perpendicular (**a**) to (D_{2h}) planar (**b**) in **I** and **II**, and in structure **III** from (D_{5h}) staggered (**a**) to (D_{5h}) eclipsed (**b**).

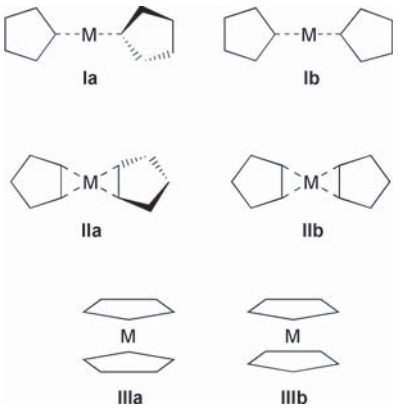

Scheme 2 N at all corners.

Computational details

A number of computational methods incorporated into the Gaussian98A7 series of programs were used in this study.[4] All geometry optimisations were carried out at the restricted Hartree–Fock (RHF), RMP2, and RB3LYP[5] levels for NaN_5,

† Electronic supplementary information (ESI) available: Table S1—selected bond lengths calculated using the 6-31G(d) basis set with various theoretical methods. See http://www.rsc.org/suppdata/p2/b1/b103852b/

KN_5, $Mg(N_5)_2$, $Ca(N_5)_2$, and $Zn(N_5)_2$. Results from both the standard split valence plus polarisation 6-31G(d) basis set and the larger 6-311+G(d) set containing diffuse functions were obtained. Additionally, the CASSCF method, which included the four highest and four lowest π molecular orbitals (MO), was employed for $Mg(N_5)_2$ and calculations using the two highest and two lowest π MOs were performed for NaN_5. As NaN_5 contains one ring and $Mg(N_5)_2$ two, these can be considered to be nearly equivalent level calculations. Stability of the restricted wavefunctions[6] was verified for all the Na and Mg structures. Normal mode analysis was performed to ascertain the nature of structures identified as stationary points on the potential energy surfaces. Vibrational frequencies reported here were not empirically scaled. For the divalent cations, RB3LYP//6-31G(d) and 6-311+G(d) calculations were carried out for the cases where one of the rings was replaced by a Cl atom placed in a linear ring–M–Cl conformation. Figures with orbitals were generated with the Molekel Program.[7]

The N atom chemical shifts were calculated according to the Gauge-Independent Atomic Orbital (GIAO) method.[8] RB3LYP//6-311++G(2d,p) level calculations were carried out on RB3LYP//6-31G(d) optimised structures. Two test cases for NaN_5 were performed to evaluate the effect of geometry change on the calculated chemical shifts by using the RB3LYP//6-311+G(d) optimised structures and by using conformer **III**. Nitromethane was used as the reference molecule and extra calculations on 1- and 2-substituted methyltetrazoles were done as a test of the theoretical method compared to the experimental.[8] Using the values for 24 N atoms in ten different azoles Witanowski *et al.*[9] found a linear relationship between the experimental results and that for Coupled Hartree–Fock (CHF)/6-31++G(d,p) of $\sigma_{exp} = (0.8804\sigma_{calc} + 112.56)$. Finally, a time dependent DFT method[10] (TD-DFT) was used to calculate the electronic transitions of MgN_5Cl, NaN_5, KN_5, CaN_5Cl and ZnN_5Cl at the 6-311+G(d) levels.

Results and discussions

In all cases, structures **II** or **IIa** were calculated to be the lowest in energy and have no negative vibrational frequency, except for Zn^{2+} where **I** or **Ia** are lowest and have no negative frequency. The relative energies in kcal mol^{-1} are reported in Table 1. The output files for all calculations in this study can be found at: http://camchem.rutgers.edu/~burke.

In all cases, the **b** structures have one more negative frequency than the **a** structures. Vector analysis (Scheme 3)

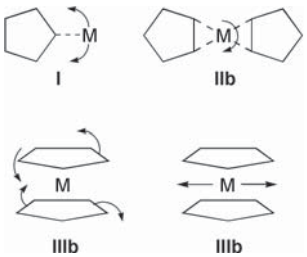

Scheme 3

shows each **b** structure to contain a rotational transition state (TS) around the cation. The negative frequency in the single ring structure **I** is an in-plane wag of the Na^+ or K^+ cation between two equivalent **II** structures. The two negative frequencies in the Mg^{2+} and Ca^{2+} **Ia** structures (**IIa** in Zn^{2+}) are due to the coupled symmetric and asymmetric combinations of the wag modes found in **I**. The three modes in **Ib** include the two for **Ia** plus the ring rotation mode also found in **IIb**. The four negative frequencies in **IIIa** correspond to two pairs of symmetry-coupled modes, the first pair for slippage of the cation between the rings and the other for movement of the rings toward structure **IIa**. The fifth negative frequency in **IIIb** is due to ring rotation from the eclipsed to staggered conformations. There are no negative frequencies for conformer **III** with Na^+ or K^+.

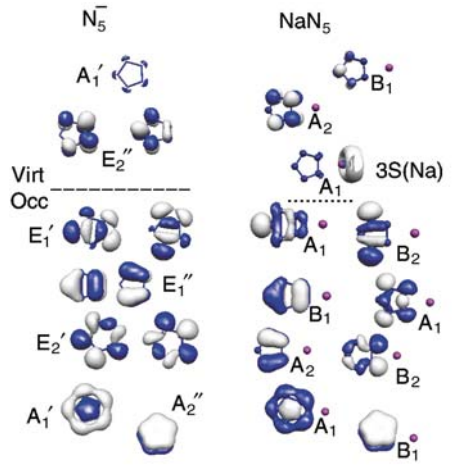

Fig. 1 Plots of eight DFT MO are given for the N_5 anion and the NaN_5 ion pair. Both sets of eight HOMOs include the five lone pair orbitals and the three p orbitals. The LUMOs of the anion consist of a degenerate pair of p MOs; while the LUMO in all ion pair cases is mainly of s character with the fourth and fifth p MO dispersed among the metals' virtual p and d orbitals. The highest shown anion MO is a low lying Rydberg orbital. D_{5h} and C_{2v} group symmetries are also given for the MOs. 6-311+G(d) basis set.

In the $(M–Cl)^+$ cases (M = Mg, Ca), the single negative frequency for **I** also corresponds to a TS between equivalent **II** structures. With M = Zn, **II** is a TS between two equivalent **I** structures. Although the **III** structure for Na, K, and M–Cl is an equilibrium structure with all positive frequencies, it is higher in energy than **II** or **I** in all cases. The relative energies range from a few kcal mol^{-1} for K and Na, *ca.* 10 for Ca, *ca.* 20 for Mg, and to over 30 for Zn. A stationary state for the **III** conformation was not found for $ZnClN_5$ using the 6-31G(d) basis set.

Inspection of Table 1 shows little effect on relative energies by differences in theoretical method used but a rather general effect by change in basis set. The DFT results for either basis set lie between those found with the RHF and RMP2 methods. Table S1 (provided as supplementary material†) gives the optimised bond lengths in Å found with the various theoretical methods and basis sets. In all methods, the presence of the cation on the side of the ring induces alternating bond lengths, thus less aromatic character.

Fig. 1 contains plots of the MOs in the anion and NaN_5 calculated with the B3LYP//6-311+(d) method. The eight highest occupied molecular orbitals of the anion consist of five lone pair orbitals, two pairs of which are degenerate, and three π orbitals of which one pair is degenerate. The D_{5h} symmetry of the anion is reduced to C_{2v} in presence of the cation in either the **I** or **II** conformation. The three lowest unoccupied molecular orbitals in the anion consist of the highest degenerate π orbitals and the $A_1'\sigma^*$ MO which resembles the lowest occupied A_1' lone pair MO but consisting of Rydberg 3p AOs with higher radial nodes (higher regions not shown on Fig. 1). The LUMO of all ion pair structures consists of the metal vacant s orbital. The vacant metal p_x, p_y, and p_z and d AO levels are interspersed with the fourth and fifth π orbitals according to the various metal cations. However, in Zn the d AOs are occupied.

The presence of the Cl atom introduces three occupied p-like orbitals making the top 11 orbitals significant to bonding. Fig. 2 shows the 11 MOs for the Zn case for both the **I** and **II** conformations, plus three of the virtual MOs. Each conformation gives a remarkably similar pattern of orbitals among

Table 1 Relative total energies (kcal mol^{-1}) for metal–pentazole complexes calculated by theoretical methods (6-31G* prime on method indicates the 6-311+G* basis set)

Metal	Method	Ia	Ib	IIa	IIb	IIIa	IIIb
Mg	RHF	9.19	9.29	0	3.90	41.88	41.92
	RHF′	7.80	7.96	0	1.04	44.27	
	MP2	15.36	15.49	0	1.30	35.54	35.54
	MP2′	12.57	12.92	0	1.59	39.58	39.77
	CAS(88)	4.80	4.91	0		70[a]	
	B3LYP	11.59	11.70	0	1.13	41.10	41.14
	B3LYP′	9.60	9.77	0	1.15	47.59	47.66
	B3LYPCl	4.74	—	0	—	19.18	—
	B3LYPCl′	3.81	—	0	—	22.68	—
Na	RHF	5.42		0		5.21	
	RHF′	4.56		0		7.04	
	MP2	6.26		0		5.30	
	MP2′	4.57		0		6.09	
	CAS(44)	4.87		0		12.46	
	CAS(44)′	4.03		0		14.53	
	B3LYP	6.11		0		5.12	
	B3LYP′	4.59		0		7.66	
K	RHF	5.45		0		2.28	
	RHF′	4.79		0		3.32	
	MP2	6.75		0		0.87	
	MP2′	5.49		0		1.55	
	B3LYP	5.99		0		2.11	
	B3LYP′	4.98		0		3.74	
Ca	RHF	19.38		0	3.90	22.43	22.44
	RHF′	18.62		0		25.92	25.94
	MP2	23.27	23.38	0	0.29	16.87	16.88
	B3LYP	21.61	21.72	0	0.45	20.52	20.51
	B3LYP′	21.05	21.24	0	1.08	26.31	26.32
	B3LYPCl	10.52	—	0	—	9.84	—
	B3LYPCl′	10.03	—	0	—	11.36	—
Zn	RHF	0	0.40	14.17	16.12	68.55	68.60
	RHF′	0		17.12		71.39	71.45
	MP2	0		13.57	16.97	73.68	73.88
	MP2′	0		14.07		67.40	67.33
	B3LYP	0	0.52	12.12	16.66	69.39	69.43
	B3LYP′	0	0.28	17.47	19.60	[a]	81.74
	B3LYPCl	0	—	7.23	—	[a]	—
	B3LYPCl′	0	—	9.88	—	39.22	—

[a] Stationary state not found, opens towards **I** or **II**.

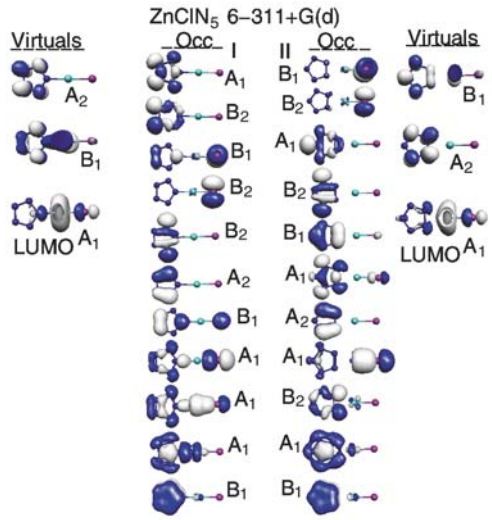

Fig. 2 The eleven DFT HOMOs and three of the unoccupied DFT MOs are given for the **I** conformation of $ZnClN_5$ (two left columns) and the **II** conformation (two right columns). C_{2v} group assignments are made for both. 6-311+G(d) basis set.

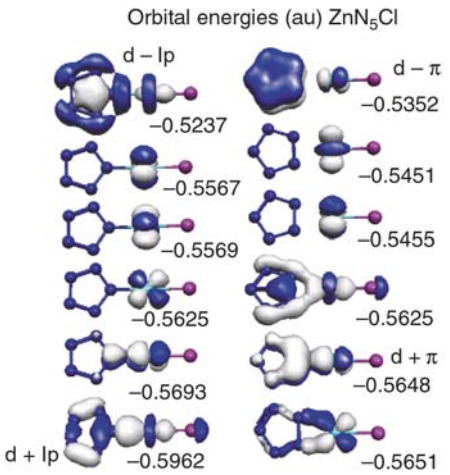

Fig. 3 Energies (au) and plots for the 6-311+G(d) DFT orbitals for $ZnClN_5$, conformation **I** in left column, **II** in right. Bottom five are the MOs with major d AO components; the top orbital in each column is displayed in Fig. 2.

all the cations. For example, the splitting of the B_1 MOs (third and seventh) in Zn (conformation **I**) is only slightly larger than that for Mg (conformation **I**), 0.0125 to 0.0110 au, respectively.

The major reason for the lower energy of the **I** conformation compared to **II** in the Zn case might be due to the combination of the occupied d orbitals with the lone pair or π orbitals. Fig. 3 gives the five d orbitals plus the combination with the lowest lone pair orbital in the **I** conformation and the five d orbitals with the lowest π orbital in the **II** conformation. There is significantly more splitting with the d_{z^2} orbital and the lone pair in the **I** conformation than with a d_{xy} orbital and the lowest π orbital in the **II** conformation.

Table 2 Vibrational frequencies (cm^{-1}) calculated with the B3LYP/6-311+G(d) method for the lowest energy configurations. The C_{2v} symmetry designations of the metal complexed pentazoles are derivatives of those of the D_{5h} pentazole anion (in parentheses)

Molecule	N_5^-	N_5^{-a}	NaN_5	KN_5	MgN_5Cl	CaN_5Cl	ZnN_5Cl
B_2 (E_1')	1239.2	1286.1	1289.2	1281.5	1305.2	1299.6	1350.3
A_1 (E_1')	1239.2	1286.1	1230.5	1232.4	1248.7	1239.8	1275.0
A_1 (A_1')	1182.0	1222.4	1216.5	1210.4	1217.2	1222.1	1218.0
B_2 (E_2')	1114.3	1124.2	1123.1	1123.0	1125.3	1123.1	1106.0
A_1 (E_2')	1114.3	1124.2	1111.8	1113.0	1104.3	1108.1	1130.2
A_1 (E_2')	995.8	1059.5	1025.3	1025.3	1036.5	1011.3	908.0
B_2 (E_2')	995.8	1059.5	980.3	988.4	953.4	973.0	1026.5
B_1 (E_2'')	767.2	782.7	766.2	765.7	756.4	756.7	731.8
A_2 (E_2'')	767.2	782.7	764.0	762.2	758.3	754.6	759.5
A_1			308.7	230.0	584.1	412.6	483.8
B_2			146.4	131.6	192.0	199.0	174.0
B_1			101.7	80.8	158.7	108.4	174.1
A_1					264.8	234.3	282.7
B_2					87.6	41.7	66.0
B_1					69.3	9.5	66.9

[a] CCSD/aug-cc-DVP ref. 2.

The calculated IR spectra for all species are marked by two strong NN stretches at ~1300 (asym, B_2) and ~1250 cm^{-1} (sym, A_1) and a prominent ring–metal atom stretch (A_1) between 600 and 200 cm^{-1}. Results for the B3LYP//6-311+G(d) method are given in Table 2. The symmetric and asymmetric stretches are similar within element groups 1 (Na, K), 2 (Mg, Ca), and 12 (Zn). The values calculated at the RB3LYP//6-31G(d) level are generally 10 cm^{-1} higher. Results for the isolated pentazole anion are similar to those reported by Bartlett *et al.*[2] calculated with the coupled cluster CCSD method with an augmented DVP basis set.

In order to calibrate the theoretical method the N atom chemical shifts were calculated for 1- and 2-methyltetrazole and compared to experiment. The results are given in Table 4. A linear regression analysis on the eight data points gives the formula $\sigma_{exp} = (1.0683\sigma_{calc} - 4.70)$ with a correlation coefficient of 0.9988. The value of the intercept −4.70 and a slope near 1.0 indicate that the B3LYP/6-311++G(2d,p) GIAO calculation on a B3LYP/6-31G(d) optimised structure gives values very close to experimental ones and much closer than those using the CHF method ($0.8804\sigma_{calc} + 112.56$).[9]

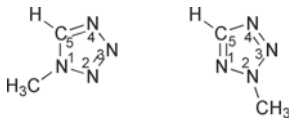

The absolute shielding value for the N atom in nitromethane is calculated to be −158.225 ppm using the B3LYP//6-311++G(2d,p) method on the B3LYP//6-31G(d) optimised structure. The theoretical value for the N atom in NH_3 is +258.440 ppm. Thus, 100.215 ppm needs to be added to the above values for comparison to external NH_3 rather than nitromethane. The reported isotropic chemical shifts in ppm were calculated as −158.225 minus the absolute shielding value calculated for each N atom in the molecule in question. There are three distinct N atoms in the **II** and **IIa** structures (also in **I** for Zn). The values in ppm for the N atom chemical shifts are reported in Table 3, using the order of closest to furthest from the metal atom to number the N atoms. As seen in Table 1, the energy differences between the **I** and **II** forms vary from 4 to 9 kcal mol^{-1}. Although this barrier might prevent intramolecular scrambling, intermolecular exchange of the metal atom in solution is expected even at low temperatures. Thus, only one NMR ^{14}N or ^{15}N signal is expected in solution.

It can be seen in Table 3 that there is very little difference in chemical shift for the $Mg(N_5)_2$ and $MgClN_5$ (**II**) species. The differences in values for atoms within the ring of the various species reflect the charge distribution. N atoms bonded to the metal have more charge and thus the chemical shifts are more negative. This effect is seen to increase for the metals in the order of K < Na ~ Ca < Mg < Zn. The much larger negative shift in Zn is most likely due to the Zn–N bond in conformation **I**.

There have been structural and mechanistic studies[3] involving ^{15}N labelling and the addition of the azide ion to the aryl diazonium ion (Scheme 4) and the recovery of the aryl azide.

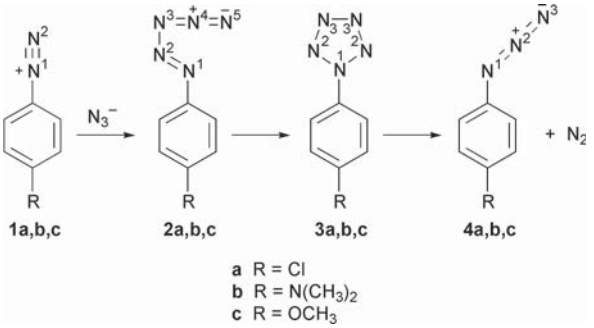

Scheme 4 Numbering for the ^{15}N atom experimental and theoretical chemical shifts.

Each study proposed a pentazole intermediate as the origin of a transitory peak in the ^{15}N spectrum. The N atom shifts have been calculated for all species in Scheme 4 and their values are reported in Table 3. For the *p*-methoxyphenyl series (**c**) the calculations indicated two rotational isomers due to restricted rotation of the aryl–oxygen bond and the mean values of the ^{15}N shifts are given in Table 3. These rotational isomers were not seen in either the proton or ^{15}N spectra. The calculations indicated rotational barriers of the order of 3 kcal mol^{-1} and hence rapid exchange between the forms would be expected. ^{15}N-Labelled samples of the compounds **1c**, **3c** and **4c** were obtained by diazotising *p*-methoxyaniline with $Na^{15}NO_2$ thereby putting a label at N2. The other ^{15}N shifts listed in Table 3 for these compounds were measured in natural abundance. The calculated ^{15}N shifts are in good agreement with the measured values except for N2 of the diazonium ion **1c** (Table 3). In this case the presence of the chloride anion in the solution is expected to increase the electron density and hence the shielding at N2. This may also account for the small increased shielding measured at N1 for the species **1c** (Table 3). The influence of the counter ion is also evident in the calculated shifts for the N_5 anions (Table 3).

The principal excitation energies (nm) and oscillator strengths (au) calculated with the TD-DFT, B3LYP//6-311+G(d) method are given in Table 5. State symmetries are given

Table 3 Theoretical (and experimental)[a] values of N atom shifts relative to external nitromethane (ppm)

Molecule	N1	N2	N3	N4	N5	NMe_2
1a	−147.4	−24.7	—	—	—	—
	(−148.3)					
1b	−132.3	−11.3	—	—	—	−277.9
1c	−142.8	−12.6	—	—	—	—
	(−)	(−61.2)[f]				
	(−147.1)[b]	(−59.7)[b]				
2a	66.5	88.9	−210.9	−144.5	−94.0	
3a	−85.3	−27.3	18.1	—	—	
	(−82.7)					
3b	−83.1	−31.3	14.0	—	—	−339.9
	(−80.0)	(−27.1)	(4.9)			(−324.6)
3c	−84.1[c]	−29.2[c]	−18.8[c]			
	(−)	(−28.1)[f]	(−)			
4a	−307.4	−146.2	−143.7	—	—	—
	(−288.1)					
4b	−312.4	−141.6	−142.9	—	—	−346.5
	(−292.2)	(−134.6)	(−146.2)			(−333.2)
4c	−310.4[c]	−144.2[c]	−144.3[c]			
	(−293.0)[d]	(−137.3)[df]	(−149.3)[d]			
	(−)	(−139.7)	(−)			
N_5Anion	−1.7	−1.7	−1.7	−1.7	−1.7	—
NaN_5 (**II**)	−28.7	3.0	14.9	—	—	—
NaN_5(**III**)	17.6	17.6	17.6	17.6	17.6	
KN_5	−18.8	2.2	15.5	—	—	—
$Mg(N_5)_2$	−48.2	6.3	24.9	—	—	—
MgN_5Cl	−47.4	5.8	23.9	—	—	—
CaN_5Cl	−27.2	6.3	29.4	—	—	—
ZnN_5Cl (**I**)	−96.1[e]	−7.9	14.5	—	—	—

[a] From ref. 3 or measured herein as indicated. [b] Measured herein in CD_3OD–D_2O (70 : 30 v/v) for natural abundance ^{15}N at 0 °C. [c] Values ±0.3. [d] Measured herein in $CDCl_3$ for natural abundance ^{15}N at probe temperature. [e] N1 in contact with Zn. [f] Measured herein in CD_3OD for ^{15}N labelled samples at −35 °C.

Table 4 Theoretical and experimental[9] values (ppm) of N atom chemical shifts for 1-methyltetrazole and 2-methyltetrazole relative to nitromethane

Substituent	Atom	DFT	Experiment
1-Methyl	1	−163.1	−159.6
	2	−6.3	−8.4
	3	34.2	23.3
	4	−41.9	−43.2
2-Methyl	1	−78.4	−73.1
	2	−107.7	−107.0
	3	9.5	3.4
	4	−42.3	−41.3

for the anion based on the D_{5h} group, as well as those based on the equivalent C_{2v} symmetries when the cations are present. Those states reported in Table 5 are of three types. The first group of six states is where the principal excitation is to the metal s AO from the four highest lone pair MOs ^{1}(ns*) and the two highest π MOs ^{1}(πs*). The next is a group of four ^{1}(nπ*) MOs and the last is a group of four ^{1}(ππ*) MOs where these named excitations are the principal excitation within that state. A 77 state TD-DFT calculation had to be done to assure that the above 14 states were all found. Other states included excitations such as from the Cl atom lone pairs or to the metal p and d virtual AOs.

The ^{1}(ππ*) transitions in the free anion are similar to those in benzene in that the lowest lying ones both involve excitations from a degenerate pair of π MOs to another degenerate pair. In benzene the D_{6h} symmetry gives an occupied e_{1g} pair and an unoccupied e_{2u} pair. The direct product of these transitions leads to three states, $B_{1u} + B_{2u} + E_{1u}$. In free pentazole anion the D_{5h} symmetry leads to a π occupied e_1'' pair and a π unoccupied e_2'' pair.

The direct product in this case is $e_1'' \times e_2'' = E_2' + E_1'$. Similarly for the four highest ^{1}(nπ*) transitions the lone pair HOMOs are an e_1' pair. This gives the direct products: $e_1' \times e_2'' = E_2'' + E_1''$. Upon distortion of one atom in the free anion to give C_{2v} symmetry or in the presence of a metal cation in the **I** or **II** conformation (*cf.* Fig. 1), the orbital degeneracies are lifted. Orbitals with e_1'' or e_2'' symmetries lead to a_2 or b_1 symmetries; the e_1' symmetry of the lone pair HOMOs lead to two lone pair MOs of a_1 and b_2 symmetries.

The ^{1}(nπ*) transitions reported here are electronically forbidden as the E_2'' and E_1'' states do not transform like an in-plane axis. This is also the case for the ^{1}(ππ*) E_2' state. The ^{1}(ππ*) E_1' state transforms like (*x,y*) and in consequence this transition is polarized in the plane of the anion, giving an oscillator strength of 0.373 au. In the presence of the cation, however, the C_{2v} group lifts the symmetry restraints on all but the new A_2 states.

The ^{1}(nπ*) transition energies vary significantly according to the metal counterion. This can also be seen at the level of the DFT orbital energies, Table 6. The orbital energy differences for Δns*, Δnπ*, and Δππ* correspond to the excitation energies calculated with the TD-DFT method. The change in the anion orbital levels induced by the presence of the metal counterion is also significant. The amount of lowering of the lone pair and π HOMOs follows the order of K < Na << Ca < Zn < Mg. Group I metals are more electropositive than group II, and K more than Na. Since Ca lies below Mg, it can be expected to interact less with the ring. The Zn atom is in the **I** conformation where the M–N distance is shorter than in the **II** conformation and thus the interaction is expected to be greater, giving the anomalous position for Zn in the series.

In summary, it is seen that the nature of the cation has an influence on the electronic, vibrational, and NMR spectra of the pentazole anion. A complex with the metal ion in the plane of the ring is energetically favoured. This induces an alternating bond length structure of C_{2v} symmetry and redistribution of charge in the anion. Further theoretical studies are in progress on the effect of solvent and on the pericyclic decomposition of the pentazole ring in the presence of a cation.

Table 5 Principal excitation energies (nm) and oscillator strengths (au) calculated with the B3LYP//6-311+G(d) method. State symmetries are given for the anion based on the D_{5h} group; those based on the equivalent C_{2v} symmetries are given in parentheses

	N_5^-	NaN_5	KN_5	MgN_5Cl	CaN_5Cl	ZnN_5Cl
^{1}(n,s*)—(A_1)	—	255.9 0.038	251.0 0.029	193.6 0.046	244.4 0.006	211.0 0.040
^{1}(n,s*)—(B_2)	—	255.5 0.001	249.9 0.001	191.8 0.002	223.8 0.003	209.0 0.02
^{1}(π,s*)—(B_1)	—	243.1 0.0.003	235.1 0.002	180.3 0.009	208.8 0.005	208.7 0.014
^{1}(n,s*)—(A_1)	—	240.0 0.045	236.8 0.023	182.8 0.045	224.2 0.000	170.2 0.004
^{1}(π,s*)—(A_2)	—	237.0 0.0	231.8 0.0	178.0 0.0	205.4 0.0	191.2 0.0
^{1}(n,s*)—(B_2)	—	208.5 0.008	208.4 0.003	172.0 0.028	174.9 0.001	194.6 0.005
^{1}(n,π*) E_2'' (A_2)[a]	188.4 0.0	197.9 0.0	197.2 0.0	205.5 0.0	213.7 0.0	183.4 0.0
^{1}(n,π*) E_2'' (B_1)[b]	188.4 0.0	197.7 0.004	197.1 0.003	204.0 0.005	209.4 0.004	218.9 0.004
^{1}(n,π*) E_1'' (B_1)[c]	186.7 0.0	188.5 0.001	184.1 0.000	185.3 0.008	192.40 0.001	176.80 0.007
^{1}(n,π*) E_1'' (A_2)[d]	186.7 0.0	187.9 0.0	182.9 0.0	184.6 0.0	189.0 0.0	215.6 0.0
^{1}(π,π*) E_2' (B_2)[e]	166.0 0.0	166.5 0.021	168.8 0.014	172.0 0.028	180.4 0.028	170.7 0.13
^{1}(π,π*) E_2'(A_1)[f]	166.0 0.0	163.5 0.042	164.0 0.017	160.5 0.009	171.5 0.041	173.9 0.169
^{1}(π,π*) E_1' (A_1)[g]	153.2 0.353	152.3 0.088	147.7 0.270	153.1 0.467	159.0[i] 0.197	186.7 0.086
^{1}(π,π*) E_1' (B_2)[h]	153.2 0.353	150.3 0.023	147.5 0.185	152.5 0.045	161.0[i] 0.085	147.6 0.462

[a] Major excitation: occupied A_1 to virtual A_2. [b] Major excitation: occupied B_2 to virtual A_2. [c] Major excitation: occupied A_1 to virtual B_1. [d] Major excitation: occupied B_2 to virtual B_1. [e] Major excitation: occupied B_1 to virtual A_2. [f] Major excitation: occupied A_2 to virtual A_2. [g] Major excitation: occupied B_1 to virtual B_1. [h] Major excitation: occupied A_2 to virtual B_1. [i] Middle state of three states containing the major excitation.

Table 6 Orbital energies and energy differences calculated with the B3LYP//6-311+G(d) method

	Anion	NaN_5	KN_5	$MgClN_5$	$CaClN_5$	$ZnClN_5$
S	—	−0.0839	−0.0683	−0.0845	−0.1033	−0.0942
HO-n	−0.1148	−0.2827	−0.2692	−0.3448	−0.3228	−0.3378
HO-π	−0.1247	−0.2981	−0.2854	−0.3701	−0.3522	−0.3544
LU-π*	+0.1864	+0.0107	+0.0341	−0.0719	−0.0670	−0.0822
ΔnS	—	0.1988	0.2009	0.2603	0.2195	0.2436
ΔπS	—	0.2142	0.2171	0.2856	0.2489	0.2602
Δnπ*	0.3012	0.2934	0.3033	0.2729	0.2558	0.2556
Δππ*	0.3111	0.3088	0.3195	0.2982	0.2852	0.2722

Acknowledgements

LAB acknowledges the National Science Foundation for a computer equipment grant MRI 9871088.

References

1 R. Huisgen and I. Ugi, *Chem. Ber.*, 1957, **90**, 2914; R. Huisgen and I. Ugi, *Chem. Ber.*, 1958, **91**, 531; for reviews see (*a*) I. Ugi *Comprehensive Heterocyclic Chemistry*, Series eds. A. R. Katritzky and C. W. Rees, Pergamon Press, Oxford, 1984, vol. 5, p. 839; (*b*) R. N. Butler, *Comprehensive Heterocyclic Chemistry II*, Series eds., A. R. Katritzky, C. W. Rees and E. F. V. Scriven, Pergamon Press, Oxford, 1996, vol. 4 (ed., R. C. Storr), p. 897.

2 M. T. Nguyen, M. Sana, G. Leroy and J. Elguero, *Can. J. Chem.*, 1983, **61**, 1435; M. T. Nguyen, M. A. McGinn, A. F. Hegarty and J. Elguero, *Polyhedron*, 1985, **4**, 1721; R. J. Bartlett, *Chem. Ind. (London)*, 2000, 140; K. F. Ferris and R. J. Bartlett, *J. Am. Chem. Soc.*, 1992, **114**, 8302.

3 R. N. Butler, A. Fox, S. Collier and L. A. Burke, *J. Chem. Soc., Perkin Trans. 2*, 1998, 2243; R. Müller, J. D. Wallis and W. von Philipsborn, *Angew. Chem., Int. Ed. Engl.*, 1985, **24**, 513.

4 Gaussian98, Revision A.7, M. J. Frisch, G. W. Trucks, H. B. Schlegel, G. E. Scuseria, M. A. Robb, J. R. Cheeseman, V. G. Zakrzewski, J. A. Montgomery, Jr., R. E. Stratmann, J. C. Burant, S. Dapprich, J. M. Millam, A. D. Daniels, K. N. Kudin, M. C. Strain, O. Farkas, J. Tomasi, V. Barone, M. Cossi, R. Cammi, B. Mennucci, C. Pomelli, C. Adamo, S. Clifford, J. Ochterski, G. A. Petersson, P. Y. Ayala, Q. Cui, K. Morokuma, D. K. Malick, A. D. Rabuck, K. Raghavachari, J. B. Foresman, J. Cioslowski, J. V. Ortiz, A. G. Baboul, B. B. Stefanov, G. Liu, A. Liashenko, P. Piskorz, I. Komaromi, R. Gomperts, R. L. Martin, D. J. Fox, T. Keith, M. A. Al-Laham, C. Y. Peng, A. Nanayakkara, C. Gonzalez, M. Challacombe, P. M. W. Gill, B. Johnson, W. Chen, M. W. Wong, J. L. Andres, C. Gonzalez, M. Head-Gordon, E. S. Replogle and J. A. Pople, Gaussian, Inc., Pittsburgh PA, 1998.

5 A. D. Becke, *Phys. Rev. A*, 1988, **38**, 3098; C. Lee, W. Yang and R. G. Parr, *Phys. Rev. B*, 1988, **37**, 785.

6 R. Seeger and J. A. Pople, *J. Chem. Phys.*, 1977, **66**, 3045; R. Bauernschmitt and R. Aldrichs, *J. Chem. Phys.*, 1996, **104**, 9047.

7 S. Portmann and H. P. Lüthi, *MOLEKEL: An Interactive Molecular Graphics Tool, Chimia*, 2000, **54**, 766.

8 K. Wolinski, J. F. Hilton and P. Pulay, *J. Am. Chem. Soc.*, 1990, **112**, 8251; J. L. Dodds, R. McWeeny and A. J. Sadlej, *Mol. Phys.*, 1980, **41**, 1419; R. Ditchfield, *Mol. Phys.*, 1974, **27**, 789.

9 M. Witanowski, Z. Biedrzycka, W. Sicinska and Z. Grabowski, *J. Magn. Reson.*, 1998, **131**, 54.

10 R. E. Stratmann, G. E. Scuseria and M. J. Frisch, *J. Chem. Phys.*, 1998, **109**, 8218; R. Bauernschmitt and R. Aldrichs, *Chem. Phys. Lett.*, 1996, **256**, 454; M. E. Casida, C. Jamorski, K. C. Casida and D. R. Salahub, *J. Chem. Phys.*, 1998, **108**, 4439.